HHS Public Access

Author manuscript

Biomacromolecules. Author manuscript; available in PMC 2019 May 14.

Published in final edited form as:

Biomacromolecules. 2018 May 14; 19(5): 1416–1424. doi:10.1021/acs.biomac.7b01311.

Effect of Ionic Functional Groups on the Oxidation State and Interfacial Binding Property of Catechol-Based Adhesive

Ameya R. Narkar, **Jonathan D. Kelley**, **Rattapol Pinnaratip**, and **Bruce P. Lee***

Department of Biomedical Engineering, Michigan Technological University, Houghton, MI 49931

Abstract

Adhesive hydrogels were prepared by copolymerizing dopamine methacrylamide (DMA) with either acrylic acid (AAc) or *N*-(3-aminopropyl)methacrylamide hydrochloride (APMH). The effect of incorporating the anionic and cationic side chains on the oxidation state of catechol was characterized using the FOX assay to track the production of hydrogen peroxide (H_2O_2) byproduct generated during the autoxidation of catechol while the interfacial binding property of the adhesive was determined by performing Johnson-Kendall-Roberts (JKR) contact mechanics tests tested over a wide range of pH values (pH 3.0-9.0). The ionic species contributed to interfacial binding to surfaces with the opposite charge, with measured work of adhesion values that were comparable to or in some cases higher than those of catechol. Addition of AAc minimized the oxidation of catechol even at a pH of 8.5 and correspondingly preserved the elevated adhesive property of catechol to both quartz and amine-functionalized surfaces. However, AAc lost its buffering capacity at pH 9.0 and catechol was oxidized at this pH. On the other hand, catechol formed cohesive covalent bond with network-bound amine side chain of APMH at a basic pH, which interfered with the interfacial binding capability of APMH and the catechol.

TOC image

*Corresponding Author: Bruce P. Lee. bplee@mtu.edu.

Supporting information

Schematic for monomers, rheometry data, additional equilibrium swelling data, schematic for H_2O_2 generation, additional H_2O_2 release data, images of adhesive hydrogels at different pH, data for W_{adh} for control D0 samples and statistical analysis.

Notes

The authors declare no competing financial interest.

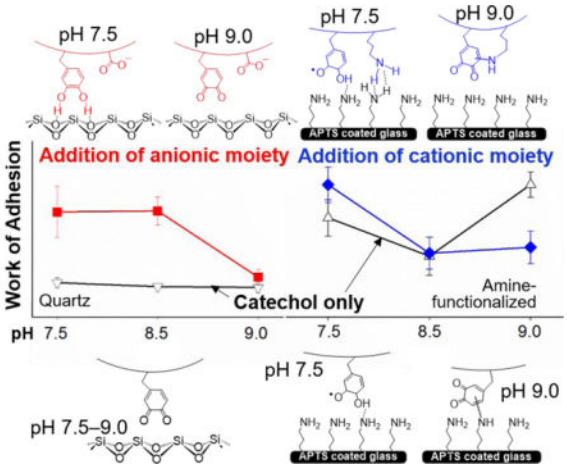

Keywords

Catechol; Cationic and anionic functional groups; Oxidation state; Wet adhesion

INTRODUCTION

Designing adhesives capable forming strong bonds to wet surfaces is critical for many biomedical and underwater marine applications.[1–3] The presence of a surface liquid layer on a substrate acts as a barrier for interfacial binding and interferes with adhesion.[4–7] Marine mussels secrete a mixture of different adhesive mussel foot proteins (mfp) to anchor themselves to a wide variety of substrates in a wet environment.[4, 8] These proteins contain a unique amino acid, L-3,4-dihydroxyphenylalanine (DOPA), which contains a catechol side chain that is responsible for moisture resistant interfacial binding. In particular, mfp-3 and 5 contain up to 30 mol % DOPA, indicating that catechol plays a major role in wet adhesion. Adhesives containing catechol functionality have hence been used to develop adhesives and coatings for various biomedical as well as industrial applications.[9–12]

The majority of existing literature focused on incorporating catechol adhesive moiety alone in designing synthetic mimics of mussel foot proteins.[4, 13, 14] However, many of the adhesive foot proteins, especially those found at the interface are highly charged (i.e., mfp-5 contains approximately 28 % cationic and 7 % anionic functional groups).[15] Recently, different research groups demonstrated that the incorporation of cationic functional groups to catechol containing adhesive enhanced its adhesive property to various inorganic surfaces (e.g., aluminum, mica, and steel) in simulated seawater or saline.[16–18] The presence of cations likely enhanced wetting to these surfaces that has a surface negative charge.[16] Additionally, the positively charged cation displaces positively charged salt ions on the surface, subsequently allowing the catechol to form stable interfacial bonds.[17] However, incorporation of anionic functional group alone did not enhance the interfacial binding property of catechol containing adhesive.[18]

While recent publications have begun to elucidate the contributions of ionic species to interfacial binding, the effect of these functional groups on the oxidation state of catechol

has yet to be systemically studied. The adhesive strength of catechol is highly dependent on its oxidation state as well as the type of surface it adheres to.[19–22] The reduced catechol is responsible for strong interfacial binding to inorganic surfaces.[23] On the other hand, catechol needs to be oxidized to its quinone form in order to participate in intermolecular covalent crosslinking with nucleophilic groups (e.g., -NH_2, -SH) found on biological substrates.[22] To counteract the basic and oxidizing environment of seawater, mussel utilize antioxidant interfacial proteins (i.e., mfp-6 and mfp-3s) to preserves the reduced state of catechol and facilitate interfacial binding.[24, 25] Similarly, the hydrophobic nature of mfp-3s as well as its ability to form self-coacervates limits catechol's contact with seawater.[26] However, adopting these strategies in the design of synthetic adhesives is challenging and potentially expensive because these strategies not only involve multiple proteins but are also dependent on a highly controlled sequence of surface deposition of these proteins. Qualitative evidence has suggested that incorporating an acidic moiety can preserve the catechol in its reduced state.[27, 28] However, there has been no systematic study that correlates the effect of ionic side chain on the oxidation state and interfacial binding property of catechol.

In this study, we determined the effect of incorporating anionic and cationic functional groups on the oxidation state of catechol. Adhesives hydrogels were prepared by copolymerizing either acrylic acid (AAc) or *N*-(3-aminopropyl)methacrylamide hydrochloride (APMH) with dopamine methacrylamide (DMA), which contain an anionic –COOH, a cationic –NH_2, and an adhesive catechol moiety, respectively. The oxidation state of catechol was characterized using ferrous ion oxidation xylenol orange (FOX) assay to track the hydrogen peroxide (H_2O_2) byproduct generated during the autoxidation of catechol. The interfacial binding property of the adhesives was determined by performing Johnson-Kendall-Roberts (JKR) contact mechanics tests on both inorganic (e.g., quartz) and organic (e.g., amine-functionalized glass) model substrates over a wide range of pH (3.0-9.0).

MATERIALS AND METHODS

Materials

APMH was purchased from Polysciences, Inc. (Warrington, PA). AAc, *N*-hydroxyethyl acrylamide (HEAA), trichloro(1H,1H,2H,2H-perfluorooctyl)silane (97 %), (3-aminopropyl) trimethoxysilane (APTS), and toluene (anhydrous, 99.8 %) were purchased from Sigma-Aldrich (St. Louis, MO). Methylene bis-acrylamide (MBAA) and 2,2-dimethoxy-2-phenylacetophenone (DMPA) were purchased from Acros Organics (New Jersey, USA). Dimethyl sulfoxide (DMSO) was purchased from Macron (Center Valley, PA), and ethanol (190 proof) was purchased from Pharmco Aaper (Brookfield, CT). DMA was synthesized following previously published protocols.[29] Glass slides were purchased from Fisher Scientific (cat. no. 12-550- A3; Hampton, NH). Quartz slides were purchased from Ted Pella (Redding, CA).

Preparation of the Coated Substrates

Amine-functionalized substrates were prepared by silane chemistry following published procedures with minor modification.[30–32] Glass slides were sonicated in acetone and

subsequently dipped into 3 v/v % APTS solution in acetone for 10 min with no agitation, 5 min with sonication and 15 min with no agitation. Slides were soaked in acetone for 10 min, dried at room temperature, and baked overnight at 60°C. To prepare hydrophobic, fluorinated glass slides for making adhesive hydrogel in the hemispherical shape, glass slides were submerged in a solution containing 0.5 mL of trichloro(1H,1H,2H,2H-perfluorooctyl)silane and 49 mL of toluene for 20 min before washing them thrice with fresh toluene, and then air dried.[33]

Preparation of the Testing Media

The acidic pH 3.0 solution was prepared by adding appropriate quantities of 1 M HCl to a solution containing 0.1 M NaCl.[33] The pH 5.0 buffer was prepared by mixing 0.1 M acetic acid and 0.1 M sodium acetate in the ratio 0.56:1. pH 7.5, 8.5 and 9.0 buffers were prepared by adjusting the pH of 10 mM Tris (hydroxymethyl)aminomethane (Tris) buffer containing 0.1 M NaCl with 1 M HCl.

Preparation of the Adhesive Hydrogel

Adhesive hydrogels were prepared by photo-curing precursor solutions containing 1 M HEAA with 10 mol % of DMA and 0 – 10 mol % of either AAc or APMH dissolved in 40% (v/v) DMSO and deionized (DI) water. The crosslinker (MBAA) and photoinitiator (DMPA) were kept constant at 3 and 0.1 mol % respectively, in relation to HEAA. Precursor solutions were degassed three times with N_2 gas, and added to a mold composed of 2 pieces of glass separated by a silicone rubber spacer (2 mm thick). To make hemispherical samples for contact mechanics tests, a maximum of 80 μL of the precursor solution was pipetted onto a hydrophobic, fluorinated glass slide. All samples were photo-cured in a ultra violet (UV) crosslinking chamber (XL-1000, Spectronics Corporation; Westbury, NY) placed inside a N_2 filled glove box (Plas laboratories; Lansing, MI) for a total of 600 s.[33–35] Immediately after curing, samples were washed in a pH 3.0 solution for overnight to remove any unreacted monomers. Samples for swelling, rheometry, and FOX assay experiments were formed into disk shape using a punch with a diameter of 10, 15, and 6.35 mm, respectively. Samples were further equilibrated at the desired pH for 24 h with constant nutation. The composition of the hydrogels was abbreviated as DxAAy where x and y stand for the mol % of DMA and AAc, respectively, or DxAPz where x and z stand for mol % of DMA and APMH, respectively. All mol % are relative to the molar concentration of HEAA. D10AA0 and D10AP0 are the same composition and will be denoted as D10 for simplicity. Similarly, the control hydrogel with no DMA and no ionic monomers was abbreviated as D0.

Equilibrium Swelling

Hydrogel discs (thickness = 2 mm and diameter = 10 mm) equilibrated at different pH levels were dried in vacuum for at least 48 h. The mass of the swollen (M_s) and dried (M_d) samples were used to calculate the equilibrium swelling ratio by using the following equation:[33]

$$\text{Equilibrium Swelling} = \frac{M_s}{M_d} \quad (1)$$

In the case of FOX assay samples, dry weights were taken into consideration to account for the effect of swelling at different pH values.

Oscillatory Rheometry

Hydrogel discs (thickness = 2 mm and diameter = 15 mm) were compressed to a constant gap of 1800 μm using a parallel plate geometry with a diameter of 20 mm. The storage modulus (G′) was measured at frequencies ranging from 0.1 – 100 Hz, and at a strain of 8 % using a TA Discovery Hybrid Rheometer-2 (TA Instruments; New Castle, DE).

FOX Assay for Quantifying Hydrogen Peroxide Concentration

The concentration of H_2O_2 generated by the adhesive hydrogel was measured using the Quantitative Peroxide Assay Kit (Thermo Scientific™; Waltham, MA).[36, 37] Hydrogel samples (thickness = 2 mm diameter = 6.35 mm) were briefly rinsed with DI water and submerged in 1000 μL of buffer solution with a desired pH at room temperature for up to 24 h. At a given time point, 20 μL of the hydrogel extract was mixed with 200 μL of the FOX assay reagent, incubated at room temperature for 15 min, and examined using a microplate reader (Synergy™ HT, BioTek; Winooski, VT) at 595 nm. 20 μL of fresh buffer solution was added back to the hydrogel extract to keep the volume of the extracting solution constant. H_2O_2 standard curve was prepared by preparing a stock solution (2000 μM of H_2O_2) from 30 % H_2O_2 solution and serially diluting it to a concentration of 7.8 – 2000 μM. H_2O_2 concentrations were normalized by the concentration of DMA as calculated based on the combined volumes of the hydrogel and the extraction fluid.

Contact Mechanics Test

Contact mechanics tests were conducted using a custom-built setup consisting of 10-g load cell (Transducer Techniques; Temecula, CA) and a miniature linear stage stepper motor (MFA-PPD, Newport; Irvine, CA).[33] Hemispherical samples equilibrated at different pH levels were affixed to an indenter (ALS-06, Transducer Techniques; Temecula, CA) using super glue (Gorilla glue or Adhesive systems MG100). Samples were compressed against the test substrate at 1 μm/sec until reaching a maximum preload of 20 mN before the samples were retracted at the same rate. Quartz or APTS-coated glass slides were used as the substrates. The surfaces were wetted with at least 25 μL of buffer solution with the same pH as those used to equilibrate the hemispheres. The force (F) versus displacement (δ) curves were integrated to determine the work of adhesion (W_{adh}), which was normalized with the calculated maximum area of contact (A_{max}) according to the following equation:[33]

$$W_{adh} = \frac{\int F \, d\delta}{A_{max}} \quad (2)$$

A_{max} was mathematically calculated by fitting the loading portion of the force vs displacement curve with the Hertzian model:[38]

$$\delta_{max} = \frac{a^2}{R}, \quad (3)$$

where δ_{max} is the maximum displacement at the maximum preload of 20 mN, a is the radius of A_{max}, and R is curvature of the hemispherical sample. The height (h) and base radius (r) of the each hemisphere were measured using digital Vernier calipers before the start of each test, to determine R:[39]

$$R = \frac{h}{2} + \frac{r^2}{2h} \quad (4)$$

A_{max} was calculated by using the following equation:

$$A_{max} = \pi a^2 \quad (5)$$

The adhesion strength (S_{adh}) was calculated by normalizing the maximum pull-off force (F_{max}) by the maximum area of contact (A_{max}) using the following equation:[40]

$$S_{adh} = \frac{F_{max}}{A_{max}} \quad (6)$$

Statistical Analysis

Statistical analysis was determined using One way analysis of variance (ANOVA) with Tukey−Kramer HSD analysis using JMP Pro 13 software (SAS Institute, NC). $p < 0.05$ was considered significant.

RESULTS AND DISCUSSION

We incorporated anionic (AAc) and cationic (APMH) functional groups into DMA containing hydrogels and tested the effect of these ionic side chains on the oxidation state and interfacial binding property of catechol (Scheme S1). Our experiments were conducted over a set of five pH values ranging from pH 3.0 to 9.0. pH levels 3.0 and 9.0 were chosen to examine the catechol at its reduced and oxidized states, respectively, and the adhesive properties of catechol under these conditions have been well characterized.[21, 33, 41] A pH of 5.0 and 7.5 were used to simulate the expected physiological pH values of tissues ranging from the acidic skin tissues to oxygenated, internal organs.[42–44] We also chose to test at pH of 8.5 because seawater pH typically ranges between 7.5 and 8.4, while natural freshwater and coastal seawater are more acidic (pH 6.5 to 8.0).[45]

Hydrogel Formation and Characterization

Prior to photo-polymerization, pH testing strips (Fisher, cat. no. 13-640-508; Hampton, NH) were used to determine the pH of the precursor solutions. While all of the formulations exhibited pH range of around 5.0 and 6.0, solutions containing 10 mol % AAc (e.g., D0AA10 and D10AA10) were highly acidic with a pH range between 2.0 and 4.0. This indicated that the carboxylate side chain of AAc drastically lowered the pH value of these solutions. Oscillatory rheology was used to verify that the hydrogels were covalently crosslinked. For all the formulation tested and regardless of incubation pH, the storage modulus (G′) values were independent of frequencies (< 45 Hz) (Figure S1) and G′ values were an order of magnitude higher than those of the loss modulus values (data not shown). These results indicated that all the samples were covalently crosslinked.[46] G′ for all the hydrogel formulations were comparable and averaged around 4–10 kPa.

Incorporating DMA into HEAA gels (i.e., D10) drastically reduced the measured swelling ratio (Figures 1 and S2), which is potentially due to π-π interactions and H-bonding between catechol moieties.[47] For D10AA10, increasing pH increased its swelling ratio as AAc (pKa ≈ 4.25)[48] became progressively more deprotonated (Figure 1). Electrostatic repulsion of the negatively charged AAc resulted in increased swelling.[48] On the other hand, D10AP10 contains APMH (pKa ≈ 10)[49] with a $–NH_2$ side chain that reduces charge density and becomes deprotonated with increasing pH, which resulted in deswelling. The swelling ratio for D10AP10 measured at pH 8.5 and higher were drastically lower when compared to those for D10. This indicated that there was an increase in the crosslinking density of the D10AP10 network potentially due to covalent crosslinking between catechol and $–NH_2$ side chain of APMH through either Michael-type addition or the formation of Schiff's base.[50, 51]

Characterizing the Oxidation State of Catechol using FOX assay

Adhesive hydrogels reported here are covalently crosslinked and insoluble, which made it difficult to employ the oft-used spectroscopy methods to directly determine the oxidation state of catechol in these samples.[41] During the autoxidation of catechol, reactive oxygen species (ROS) such as superoxide ($O_2^{\bullet -}$) and hydrogen peroxide (H_2O_2) are generated as byproducts (Scheme S2).[37] Dismutation of $O_2^{\bullet -}$ also generates H_2O_2, which is significantly more stable when compared to $O_2^{\bullet -}$.[52] As such, H_2O_2 can be quantified using the conventional FOX assay as it is being generated and released from the hydrogel samples.

Tracking the concentration of H_2O_2 over time provided a convenient approach for determining the oxidation state of catechol in our samples at different pH values. D10 incubated at pH 3.0 and 5.0 did not generate H_2O_2 even after 24 h (Figures 2 and S3) and these samples remained clear and colorless (Table S1). As expected, catechol remained in its reduced state in an acidic pH.[23] However, when the pH was raised to 7.5, D10 generated detectable amount of H_2O_2 within 2 h and the H_2O_2 concentration continued to increase for 24 h (0.0481 ± 0.00373 μM H_2O_2/μM catechol by 24 h), indicating that catechol were increasingly oxidized over time. Given the half-life of H_2O_2 at room temperature (≈ pH 7.0) can range from 12 – 30 h,[53] D10 continued to generate H_2O_2 over time. D10 generated more H_2O_2 when these samples were incubated at a more basic pH (1.5 and 1.9 fold increase at pH 8.5 and 9.0, respectively, when compared to pH 7.5). These samples also turned brown

when incubated at a pH of 7.5 and higher, which is an indication of catechol oxidation (Table S1). Catechol becomes increasingly more oxidized when the pH of the solution approach the pK_a of catechol (≈ 9.3).[54]

When AAc was incorporated, D10AA10 did not generate H_2O_2 even when it was incubated at pH 7.5 and only a small amount of H_2O_2 was detected at pH 8.5 (Figure 2). Correspondingly, D10AA10 remained colorless when incubated at a pH that was 7.5 or less and D10AA10 only developed minor discoloration around its edge after it was incubated at pH 8.5 for 24 h (Table S1). When the pH was raised to 9.0, a significantly higher amount of H_2O_2 was generated (0.0617 ± 0.00202 μM H_2O_2/μM catechol after 24 h) and D10AA10 appeared brown in color (Table S1), indicating catechol oxidation. However, the amount of H_2O_2 generated from D10AA10 was 1.5 fold lower compared to that of D10 tested at the same pH. These results suggest that the carboxyl side chain of AAc buffered the local pH within the adhesive network and contributed to maintaining the reduced form of catechol. Precursor solutions containing AAc (e.g., D0AA10 and D10AA10) were also significantly more acidic (pH 2.0-4.0) when compared to those (e.g., D0, D10, D10AP10, etc.) that do not contain AAc (pH 5.0-6.0). However, AAc lost its buffering capacity when the surrounding media was highly basic.

Samples containing APMH (e.g., D10AP10) generated similar amount of H_2O_2 as D10 at pH levels between 3.0 and 7.5 (Figure 2). At a more basic pH, D10AP10 generated higher amount of H_2O_2 when compared to D10 (2.5 and 3 fold increase at pH 8.5 and 9.0, respectively). Previously, we reported that dopamine with a free $–NH_2$ group generated significantly more H_2O_2 when compared to DMA, potentially due to the polymerization of dopamine to form polydopamine.[37] Autoxidation of dopamine involves intracyclization and formation of intramolecular Michael-type adduct to form dopamine indole.[11] On the other hand, the primary amine group in DMA was functionalized with a methacrylamide and was unavailable for covalent crosslinking. This increase in the measured H_2O_2 from D10AP10 may be attributed to covalent crosslinking between the $–NH_2$ of APMH and oxidized quinone.

The measured H_2O_2 concentration was lower than the concentration of catechol in the hydrogel network. While H_2O_2 was constantly being generated, H_2O_2 decomposition also occurred concurrently. Additionally, the hydrogel network also served as a cage that hinders the diffusion of H_2O_2 into the extracting solution.[36, 37] Nevertheless, H_2O_2 quantification served as useful approach to measure the extent of catechol oxidation *in situ*. Samples that did not contain DMA (e.g., D0, D0AA10 and D0AP10) did not generate H_2O_2 over 24 h for all the pH values (data not shown) and these samples remained colorless (Table S1), confirming that the source of H_2O_2 is associated with autoxidation of catechol.

Contact Mechanics Tests

JKR contact mechanics test was performed to assess the effect of incorporating AAc and APMH on the interfacial binding property of catechol to two types of surfaces (e.g., quartz and APTS-coated glass). Quartz was used as a model inorganic surface as silica-based materials are commonly used as medical and dental implants,[55, 56] while APTS-coated glass

was used to simulate amine functional group found on tissue surfaces.[57] Most importantly, interaction between catechol and these surfaces have been well documented.[22, 23]

Adhesion to Quartz Surface

The control HEAA hydrogels (D0) exhibited weak adhesion to quartz surface with W_{adh} values that averaged around 11-130 mJ/m^2 depending on the pH (Table S2). Addition of DMA to HEAA hydrogels (D10) significantly increased W_{adh} values and D10 demonstrated elevated adhesive property at acidic pH (444.7 ± 123.7 mJ/m^2 at pH 3.0; Figure 3a). This is due to the strong interfacial binding (i.e., H-bond) between catechol and SiO_2 surface (Scheme 1a).[33, 58] W_{adh} values for D10 were greatly reduced at a pH of 7.5 or higher (90 % reduction when compared to pH 3.0) as a result of catechol oxidation. Addition of an anionic monomer, AAc, to HEAA hydrogels (D0AA10) showed negligible W_{adh} value over the entire range of pH values except some weak interactions at pH 3.0. With increasing pH, both- the –COOH group of AAc and the quartz surface become highly negatively charged[59, 60] and electrostatic repulsion between D0AA10 and quartz surface greatly minimized the measured adhesion values (Scheme 1b).

When AAc was incorporated into DMA-containing hydrogel (D10AA10), there was a drastic increase in the measured W_{adh} values at pH 7.5 and 8.5 when compared to those of D10 (~ 7 and 11 fold increase, respectively) (Figure 3a). Given that D0AA10 was poorly adhesive to quartz at this pH range, the elevated adhesive values measured for D10AA10 can be attributed to catechol's ability to from strong interfacial bonds (Scheme 1c). The W_{adh} values measured at pH 7.5 and 8.5 were not significantly different from the value measured at pH 5.0 (Table S5). The presence of AAc likely maintained catechol in its reduced and adhesive state in a neutral to mildly basic pH, which was confirmed by the FOX assay results (Figure 2) and the photographs of the hydrogel (Table S1). The adhesive property of D10AA10 was drastically diminished at pH 9.0 as a result of catechol oxidation, as the basic buffer overcame the buffering capacity of AAc. The FOX assay data also supported this as the measured concentration of H_2O_2 was the highest at pH 9.0. Our data confirmed previously published results that indicated anions do not actively participate in interfacial binding to inorganic surfaces.[18] However, our new findings suggest that the anionic functional groups contributed by buffering the local pH to preserve the adhesive property of catechol.

Adding a cationic monomer, APMH, to HEAA hydrogels (D0AP10) resulted in W_{adh} values (200-380 mJ/m^2) that were comparable to those of D10 (452.6 ± 58.18 mJ/m^2 at pH 3.0; Figure 3b). This result is in agreement with previous findings that indicated cationic functional groups contributed significantly to interfacial binding to inorganic surfaces.[16–18] APMH likely interacted with the quartz surface using a combination of electrostatic interaction and H-bonding (Scheme 1d). The W_{adh} values for D10AP10 mirrored those of D0AP10 for pH between 3.0 and 7.5. There was no additive effect with the addition of both catechol and $–NH_2$ into the adhesive network. Most noticeably, W_{adh} values for D10AP10 was more than 10 fold higher when compared to that observed for D10 at pH 7.5. Based on the FOX assay, both D10 and D10AP10 produced equivalent amount of H_2O_2 over 24 h (Figure 2), indicating that catechol in both adhesives were equally oxidized. The elevated

adhesive property demonstrated by D10AP10 was likely contributed by the presence of –NH_2 side chain of APMH. With further increase in pH (i.e., pH 8.5 and 9.0), W_{adh} values for D10AP10 decreased drastically and became equivalent to those of oxidized D10. However, W_{adh} values for D0AP10 remained constant and average around 300-380 mJ/m^2. These results indicated that the oxidized catechol in D10AP10 likely formed covalent crosslinks with –NH_2 of APMH, leading to reduced availability of APMH for interfacial binding (Scheme 1e). This observation is in agreement with the FOX assay data, which also showed that D10AP10 generated significantly higher amount of H_2O_2 at pH 8.5 and 9.0 as compared to D10, possibly due to the formation of adducts with the nucleophile.[37] S_{adh} data (Figures S4a and S4b, Tables S9-S11) was largely in agreement with the W_{adh} results.

Adhesion to –NH_2-functionalized Glass

W_{adh} values for D10 decreased with increasing pH (W_{adh} = 471.7 ± 138.5 and 107.6 ± 62.11 mJ/m^2 for pH 3.0 and 8.5, respectively.) (Figure 4a). The strong interaction at acidic pH was due to the strong cation-π interactions between catechol and the positively charged APTS substrate (Scheme 2a).[8, 14] This interaction may have weakened as the pH was increased due to reduced surface charge density and the deprotonation of –NH_2. D10 may have transitioned to form weaker H-bond or electrostatic interactions. Interestingly, elevated W_{adh} value was obtained for D10 at pH 9.0 (W_{adh} = 340.0 ± 41.15 mJ/m^2), which suggested the formation of interfacial covalent bond formation between oxidized quinone and primary amine on the surface.[23]

W_{adh} for hydrogel containing only the anionic AAc (i.e., D0AA10) initially increased with increasing pH reaching a maximum at pH 5.0 (W_{adh} = 343.1 ± 13.93 mJ/m^2; Figure 4a, Scheme 2b). At pH 3.0, the carboxyl group of AAc was mostly protonated and interacted weakly with APTS through H-bonding. When the solution pH exceeded the dissociation constant of AAc (pKa ≈ 4.25),[48] the carboxyl group became more negatively charged and interacted with APTS through electrostatic interaction. However, further increase in pH resulted in reduced W_{adh} values as the surface positive charge density decreased and APTS becomes progressively more deprotonated. Nevertheless, AAc demonstrated considerable amount of adhesion to APTS-functionalized surface and outperformed catechol at pH 7.5 and 8.5.

When both DMA and AAc were introduced into HEAA (D10AA10), both functional groups (i.e., catechol and carboxylate group) appeared to interact synergistically with the APTS surface, as the measured W_{adh} values were significantly higher than the formulations containing either of the two functional groups alone (i.e., D10 or D0AA10; Figure 4a). The W_{adh} values measured in this series were also the highest among the adhesive-surface combinations that were investigated in this study (i.e., W_{adh} = 658.5 ± 141.9 mJ/m^2 at pH 3.0). The combination of cation-π and electrostatic interactions likely contributed to the elevated adhesive property (Scheme 2c). While the W_{adh} values for both D10 and D0AA10 decreased with increasing pH, W_{adh} values for D10AA10 did not change significantly with changing pH (Table S8). Based on FOX assay results, addition of AAc preserved the reduced state of catechol at pHs 5.0-8.5, which suggest that catechol in its reduced form is required for strong interaction with –NH_2-functionalized surface. Additionally, long range

interaction (i.e., electrostatic attraction between $–COO^-$ and $–NH_3^+$) likely promoted catechol surface adsorption, potentially similar to how cations promoted adhesion of catechol adsorption to inorganic substrates.[61] When the pH was raised to 9.0, D10AA10 exhibited W_{adh} of 429.1 ± 55.45 mJ/m^2 even though AAc lost its buffering capacity at this pH. Similar to D10, the elevated adhesion values is likely resulted from the formation of interfacial covalent bond.[23]

Both D0AP10 and APTS-functionalized surface contained $–NH_2$ functional groups, which were positively charged at an acidic pH. Electrostatic repulsion between the hydrogel and surface resulted in reduced interaction at pH 3.0 (W_{adh} = 36.23 ± 22.38 mJ/m^2; Figure 4b, Scheme 2d). W_{adh} value increased with increasing pH as the charge density for both the adhesive and substrate decreased, resulting in increased interfacial binding. Specifically, at pH 9.0, the interfacial binding was the strongest (W_{adh} = 402.0 ± 23.64 mJ/m^2) potentially due to interfacial H-bond formation.

At pH 3.0 and 5.0, D10AP10 exhibited comparable W_{adh} values as D10 (Figure 4b). This indicated that catechol needed to form strong interfacial cation-π interactions while overcoming electrostatic repulsion between network bound $–NH_3^+$ of APMH and positively charged surface ($–NH_3^+$ of APTS; Scheme 2e). As the pH was increased to 7.5, W_{adh} value for D10AP10 averaged around 339.7 ± 57.07 mJ/m^2, which was ~ 1.5 fold higher compared to those of D10 and D0AP10. With increasing pH, a reduction in charge density allowed both catechol and network-bound $–NH_2$ group to from interfacial bonds. However, further increase in the pH resulted in a statistically significant decrease in interfacial binding (W_{adh} at pH 8.5 = 117.3 ± 51.59 mJ/m^2 and pH 9.0 = 136.4 ± 52.95 mJ/m^2) (Table S8). This is possibly due to the cohesive crosslinking between network-bound–NH_2 of APMH and quinone,[50, 51] resulting in reduced availability of APMH and catechol at pH 8.5 and 9.0, respectively, for interacting with the amine functionalized surface. S_{adh} data (Figures S4c and S4d, Tables S12-S14) was largely in agreement with W_{adh} data.

Taken together, both anionic and cationic functional groups contributed considerably to interfacial binding through electrostatic attraction to surfaces with the opposite charges. Measured W_{adh} values for these ionic species were comparable to and in some cases exceeded those measured for catechol. Most noticeably, the carboxylate side chain of AAc buffered local pH to preserve the reduced state of catechol, which was critical for binding to both quartz and $–NH_2$-functionalized surfaces. Unlike strategies devised by marine mussels that require multiple foot proteins with unique features (i.e., antioxidant property, surface drying property, etc.) to preserve the reduced and adhesive state of catechol,[24, 26] adding anionic functional group provided a simple yet effective approach in designing synthetic mussel-mimetic adhesives for applications suitable for mildly basic conditions. On the other hand, the $–NH_2$ side chain of APMH promoted cohesive crosslinking with oxidized quinone in a basic pH, which limited interfacial interactions. Although we did not test adhesives that combined both ionic species; natural interfacial foot proteins (i.e., mfp-5 and mfp-3) containing both anionic and cationic functional groups[25, 62] and synthetic mimics that contain both species have demonstrated enhanced adhesion under simulated seawater conditions.[18] The anionic and cationic side chains in these adhesives likely contributed synergistically to interfacial binding by separately preserving the reduced state of catechol

and promoting adhesion to inorganic surfaces (i.e., electrostatic interaction, repelling surface anions), respectively. The adhesion testing described here consisted of a soft hydrogel contacting a rigid substrate and additional testing is required to determine if the same trends can be obtained for contacting a soft, compliant substrate (i.e., soft tissue).[63] Finally, our report provided a useful guide for designing synthetic adhesives and coatings depending on the intended application (i.e., different surface type and pH).

CONCLUSIONS

In this study, we systemically evaluated the effect of incorporating anionic (AAc) and cationic (APMH) functional groups on catechol adhesion to both model inorganic and organic surfaces across a wide range of pH levels. Specifically, we correlated the effect of these ionic species on the oxidation state and interfacial binding property of catechol. Both ionic functional groups contributed considerably to interfacial binding through electrostatic attraction to surfaces with the opposite charges. In some situations, measured adhesion values for these ionic species were comparable to and can exceed those of catechol. Addition of AAc preserved the reduced and adhesive form of catechol in a mildly basic condition. On the other hand, the $–NH_2$ of APMH resulted in covalent crosslinking between oxidized quinone in a basic pH, which interfered with interfacial binding.

Supplementary Material

Refer to Web version on PubMed Central for supplementary material.

Acknowledgments

We thank Randall Wilharm for the synthesis of DMA.

Funding Sources

This project was supported by the Office of Naval Research Young Investigator Award under Award Number N00014-16-1-2463, the National Institutes of Health under Award Number R15GM104846, and the Portage Health Foundation. R.P. was supported by the Royal Thai Government Scholarship.

References

1. Stewart RJ. Protein-based underwater adhesives and the prospects for their biotechnological production. Appl Microbiol Biotechnol. 2011; 89(1):27–33. [PubMed: 20890598]
2. Deming TJ. Synthetic polypeptides for biomedical applications. Prog Polym Sci. 2007; 32(8):858–875.
3. Bordes M, Davies P, Cognard JY, Sohier L, Sauvant-Moynot V, Galy J. Prediction of long term strength of adhesively bonded steel/epoxy joints in sea water. Int J Adhes Adhes. 2009; 29(6):595–608.
4. Lee BP, Messersmith PB, Israelachvili JN, Waite JH. Mussel-inspired adhesives and coatings. Annual review of materials research. 2011; 41:99–132.
5. Waite JH. Nature's underwater adhesive specialist. Int J Adhes Adhes. 1987; 7(1):9–14.
6. Wilker JJ. Positive charges and underwater adhesion. Science. 2015; 349(6248):582–583. [PubMed: 26250668]
7. Comyn, J. The relationship between joint durability and water diffusion. Applied Science Publishers; London: 1981.

8. Lu Q, Danner E, Waite JH, Israelachvili JN, Zeng H, Hwang DS. Adhesion of mussel foot proteins to different substrate surfaces. Journal of The Royal Society Interface. 2013; 10:20120759.
9. Yamamoto H. Marine adhesive proteins and some biotechnological applications. Biotechnology and Genetic Engineering Reviews. 1996; 13(1):133–166. [PubMed: 8948111]
10. Meredith HJ, Wilker JJ. The interplay of modulus, strength, and ductility in adhesive design using biomimetic polymer chemistry. Adv Funct Mater. 2015; 25(31):5057–5065.
11. Lee H, Dellatore SM, Miller WM, Messersmith PB. Mussel-Inspired Surface Chemistry for Multifunctional Coatings. Science. 2007; 318(5849):426–430. [PubMed: 17947576]
12. Brubaker CE, Messersmith PB. The Present and Future of Biologically Inspired Adhesive Interfaces and Materials. Langmuir. 2012; 28(4):2200–2205. [PubMed: 22224862]
13. Faure E, Falentin-Daudré C, Jérôme C, Lyskawa J, Fournier D, Woisel P, Detrembleur C. Catechols as versatile platforms in polymer chemistry. Progress in Polymer Science. 2013; 38(1):236–270.
14. Kord Forooshani P, Lee BP. Recent approaches in designing bioadhesive materials inspired by mussel adhesive protein. J Polym Sci Part A: Polym Chem. 2017; 55:9–33.
15. Waite JH, Housley TJ, Tanzer ML. Peptide repeats in a mussel glue protein: theme and variations. Biochemistry. 1985; 24(19):5010–5014. [PubMed: 4074674]
16. White JD, Wilker JJ. Underwater bonding with charged polymer mimics of marine mussel adhesive proteins. Macromolecules. 2011; 44(13):5085–5088.
17. Maier GP, Rapp MV, Waite JH, Israelachvili JN, Butler A. Adaptive synergy between catechol and lysine promotes wet adhesion by surface salt displacement. Science. 2015; 349(6248):628–632. [PubMed: 26250681]
18. Clancy SK, Sodano A, Cunningham DJ, Huang SS, Zalicki PJ, Shin S, Ahn BK. Marine Bioinspired Underwater Contact Adhesion. Biomacromolecules. 2016; 17(5):1869–1874. [PubMed: 27046671]
19. Yu M, Hwang J, Deming TJ. Role of l-3,4-Dihydroxyphenylalanine in Mussel Adhesive Proteins. J Am Chem Soc. 1999; 121(24):5825–5826.
20. Lee BP, Chao CY, Nunalee FN, Motan E, Shull KR, Messersmith PB. Rapid Gel Formation and Adhesion in Photocurable and Biodegradable Block Copolymers with High DOPA Content. Macromolecules. 2006; 39(5):1740–1748.
21. Yu J, Wei W, Menyo MS, Masic A, Waite JH, Israelachvili JN. Adhesion of Mussel Foot Protein-3 to TiO2 Surfaces: the Effect of pH. Biomacromolecules. 2013; 14(4):1072–1077. [PubMed: 23452271]
22. Guvendiren M, Messersmith PB, Shull KR. Self-Assembly and Adhesion of DOPA-Modified Methacrylic Triblock Hydrogels. Biomacromolecules. 2008; 9(1):122–128. [PubMed: 18047285]
23. Lee H, Scherer NF, Messersmith PB. Single-molecule mechanics of mussel adhesion. Proceedings of the National Academy of Sciences. 2006; 103(35):12999–13003.
24. Yu J, Wei W, Danner E, Ashley RK, Israelachvili JN, Waite JH. Mussel protein adhesion depends on interprotein thiol-mediated redox modulation. Nature chemical biology. 2011; 7(9):588–590. [PubMed: 21804534]
25. Wei W, Tan Y, Martinez Rodriguez NR, Yu J, Israelachvili JN, Waite JH. A mussel-derived one component adhesive coacervate. Acta Biomaterialia. 2014; 10(4):1663–1670. [PubMed: 24060881]
26. Wei W, Yu J, Broomell C, Israelachvili JN, Waite JH. Hydrophobic enhancement of dopa-mediated adhesion in a mussel foot protein. J Am Chem Soc. 2012; 135(1):377–383. [PubMed: 23214725]
27. Moulay S, Mehdaoui R. Hydroquinone/catechol-bearing polyacrylic acid: redox polymer. React Funct Polym. 2004; 61(2):265–275.
28. Wang W, Xu Y, Li A, Li T, Liu M, von Klitzing R, Ober CK, Kayitmazer AB, Li L, Guo X. Zinc induced polyelectrolyte coacervate bioadhesive and its transition to a self-healing hydrogel. Rsc Advances. 2015; 5(82):66871–66878.
29. Lee H, Lee BP, Messersmith PB. A reversible wet/dry adhesive inspired by mussels and geckos. Nature. 2007; 448(7151):338–341. [PubMed: 17637666]
30. Kiernan J. Strategies for preventing detachment of sections from glass slides. Micros Today. 1999; 99(96):22–24.

31. Chandradoss SD, Haagsma AC, Lee YK, Hwang JH, Nam JM, Joo C. Surface passivation for single-molecule protein studies. Journal of visualized experiments: JoVE. 2014; (86):50549.
32. Taglietti A, Arciola CR, D'Agostino A, Dacarro G, Montanaro L, Campoccia D, Cucca L, Vercellino M, Poggi A, Pallavicini P. Antibiofilm activity of a monolayer of silver nanoparticles anchored to an amino-silanized glass surface. Biomaterials. 2014; 35(6):1779–1788. [PubMed: 24315574]
33. Narkar AR, Barker B, Clisch M, Jiang J, Lee BP. pH Responsive and Oxidation Resistant Wet Adhesive based on Reversible Catechol–Boronate Complexation. Chem Mater. 2016; 28(15): 5432–5439. [PubMed: 27551163]
34. Lee BP, Konst S. Novel hydrogel actuator inspired by reversible mussel adhesive protein chemistry. Adv Mater. 2014; 26(21):3415–3419. [PubMed: 24596273]
35. Lee BP, Lin M-H, Narkar A, Konst S, Wilharm R. Modulating the movement of hydrogel actuator based on catechol–iron ion coordination chemistry. Sensors and Actuators B: Chemical. 2015; 206:456–462.
36. Meng H, Liu Y, Lee BP. Model polymer system for investigating the generation of hydrogen peroxide and its biological responses during the crosslinking of mussel adhesive moiety. Acta Biomater. 2017; 48:144–56. [PubMed: 27744069]
37. Meng H, Li Y, Faust M, Konst S, Lee BP. Hydrogen Peroxide Generation and Biocompatibility of Hydrogel-Bound Mussel Adhesive Moiety. Acta biomaterialia. 2015; 17:160–169. [PubMed: 25676582]
38. Hertz H. On the contact of elastic solids. J Reine Angew Math. 1881; 92:156–171.
39. Shull KR, Chen WL. Fracture mechanics studies of adhesion in biological systems. Interface Sci. 2000; 8(1):95–110.
40. Burkett JR, Wojtas JL, Cloud JL, Wilker JJ. A Method for Measuring the Adhesion Strength of Marine Mussels. The Journal of Adhesion. 2009; 85(9):601–615.
41. Cencer M, Liu Y, Winter A, Murley M, Meng H, Lee BP. Effect of pH on the Rate of Curing and Bioadhesive Properties of Dopamine Functionalized Poly(ethylene glycol) Hydrogels. Biomacromolecules. 2014; 15(8):2861–2869. [PubMed: 25010812]
42. Ohman H, Vahlquist A. In vivo studies concerning a pH gradient in human stratum corneum and upper epidermis. Acta dermatovenereologica-stockholm. 1994; 74:375–379.
43. Waugh, A., Grant, A. Ross & Wilson Anatomy and Physiology in Health and Illness E-Book. Elsevier Health Sciences; 2010.
44. Zhang, S., Soller, BR. In-vivo determination of myocardial pH during regional ischemia using near-infrared spectroscopy. Vol. 1998. SPIE Proc; 1998. p. 110-117.
45. Chester, R., Jickells, T. Marine Geochemistry. Wiley-Blackwell Publishing; 2012.
46. Li Y, Meng H, Liu Y, Narkar A, Lee BP. Gelatin Microgel Incorporated Poly(ethylene glycol)-Based Bioadhesive with Enhanced Adhesive Property and Bioactivity. ACS Applied Materials & Interfaces. 2016; 8(19):11980–11989. [PubMed: 27111631]
47. Min Y, Hammond PT. Catechol-modified polyions in layer-by-layer assembly to enhance stability and sustain release of biomolecules: a bioinspired approach. Chem Mater. 2011; 23(24):5349–5357.
48. Jin X, Hsieh YL. pH-responsive swelling behavior of poly (vinyl alcohol)/poly (acrylic acid) bi-component fibrous hydrogel membranes. Polymer. 2005; 46(14):5149–5160.
49. Hu X, Tong Z, Lyon LA. Synthesis and physicochemical properties of cationic microgels based on poly (N-isopropylmethacrylamide). Colloid Polym Sci. 2011; 289(3):333–339.
50. Yang J, Saggiomo V, Velders AH, Stuart MAC, Kamperman M. Reaction Pathways in Catechol/Primary Amine Mixtures: A Window on Crosslinking Chemistry. PloS one. 2016; 11(12):e0166490. [PubMed: 27930671]
51. Yang J, Stuart MAC, Kamperman M. Jack of all trades: versatile catechol crosslinking mechanisms. Chem Soc Rev. 2014; 43(24):8271–8298. [PubMed: 25231624]
52. Bokare AD, Choi W. Singlet-oxygen generation in alkaline periodate solution. Environmental science & technology. 2015; 49(24):14392–14400. [PubMed: 26594871]

53. Tort M, Fletcher C, Wooster G, Bowser P. Stability of hydrogen peroxide in aquaria as a fish disease treatment. Journal of applied aquaculture. 2004; 14(3–4):37–45.
54. Springsteen G, Wang B. A detailed examination of boronic acid–diol complexation. Tetrahedron. 2002; 58(26):5291–5300.
55. Fu Q, Rahaman MN, Fu H, Liu X. Silicate, borosilicate, and borate bioactive glass scaffolds with controllable degradation rate for bone tissue engineering applications. I. Preparation and in vitro degradation. Journal of Biomedical Materials Research Part A. 2010; 95(1):164–171. [PubMed: 20544804]
56. Lee SB, González-Cabezas C, Kim KM, Kim KN, Kuroda K. Catechol-Functionalized Synthetic Polymer as a Dental Adhesive to Contaminated Dentin Surface for a Composite Restoration. Biomacromolecules. 2015; 16(8):2265–2275. [PubMed: 26176305]
57. Kaushik N, Kaushik N, Pardeshi S, Sharma J, Lee S, Choi E. Biomedical and Clinical Importance of Mussel-Inspired Polymers and Materials. Marine Drugs. 2015; 13(11):6792–6817. [PubMed: 26569266]
58. Chung H, Glass P, Pothen JM, Sitti M, Washburn NR. Enhanced Adhesion of Dopamine Methacrylamide Elastomers via Viscoelasticity Tuning. Biomacromolecules. 2011; 12(2):342–347. [PubMed: 21182292]
59. Nesrinne S, Djamel A. Synthesis, characterization and rheological behavior of pH sensitive poly (acrylamide-co-acrylic acid) hydrogels. Arabian Journal of Chemistry. 2017; 10(4):539–547.
60. Tombácz E, Szekeres M. Colloidal behavior of aqueous montmorillonite suspensions: the specific role of pH in the presence of indifferent electrolytes. Applied Clay Science. 2004; 27(1):75–94.
61. Wei W, Yu J, Gebbie MA, Tan Y, Martinez Rodriguez NR, Israelachvili JN, Waite JH. Bridging Adhesion of Mussel-Inspired Peptides: Role of Charge, Chain Length, and Surface Type. Langmuir. 2015; 31(3):1105–1112. [PubMed: 25540823]
62. Seo S, Das S, Zalicki PJ, Mirshafian R, Eisenbach CD, Israelachvili JN, Waite JH, Ahn BK. Microphase Behavior and Enhanced Wet-Cohesion of Synthetic Copolyampholytes Inspired by a Mussel Foot Protein. J Am Chem Soc. 2015; 137(29):9214–9217. [PubMed: 26172268]
63. Cholewinski A, Yang FK, Zhao B. Underwater Contact Behavior of Alginate and Catechol-Conjugated Alginate Hydrogel Beads. Langmuir. 2017; 33(34):8353–8361. [PubMed: 28787168]

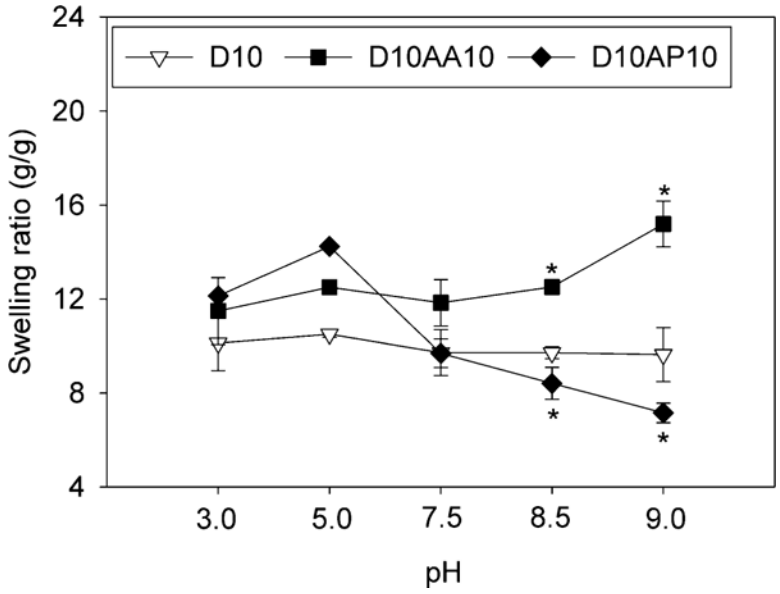

Figure 1.

Swelling ratios of adhesive hydrogels equilibrated at pH 3.0-9.0 for 24 h (n = 3). * $p < 0.05$ when compared to D10 at the same pH.

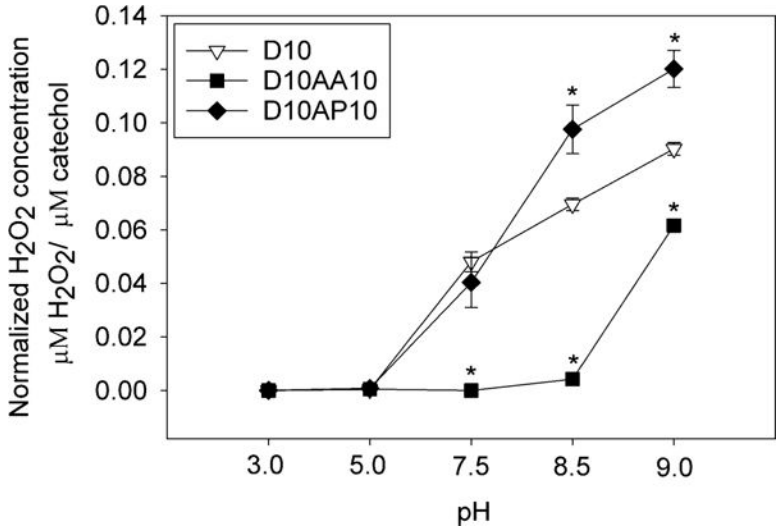

Figure 2.

Normalized concentration of H_2O_2 released from hydrogels equilibrated at pH 3.0-9.0 after 24 h of incubation (n = 3). * $p < 0.05$ when compared to D10 at the same pH.

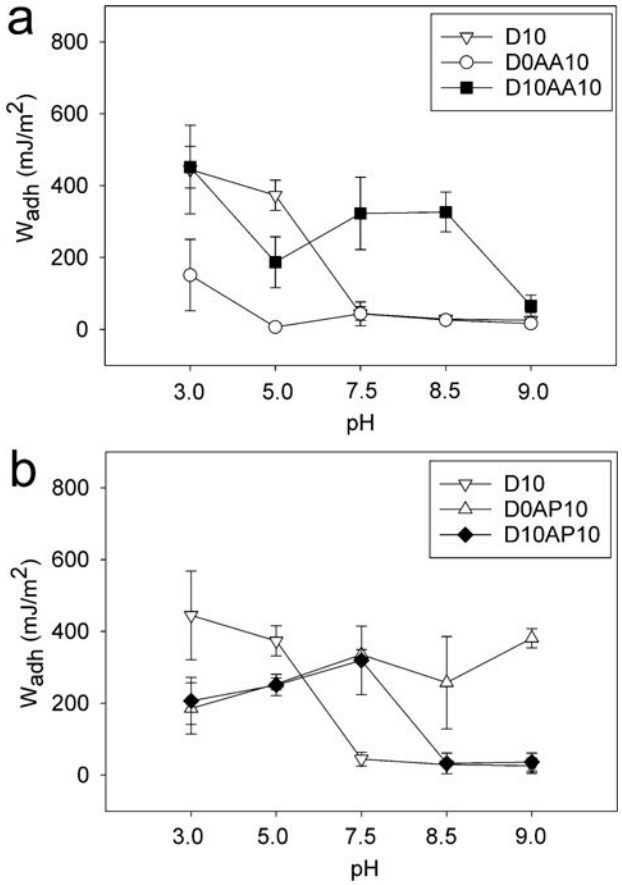

Figure 3.

Work of adhesion (W_{adh}) for adhesive hydrogels containing anionic AAc (a) and cationic APMH (b) tested against a wetted quartz substrate at pH 3.0-9.0 (n = 3). Refer to Tables S3-S5 for results of statistical analysis.

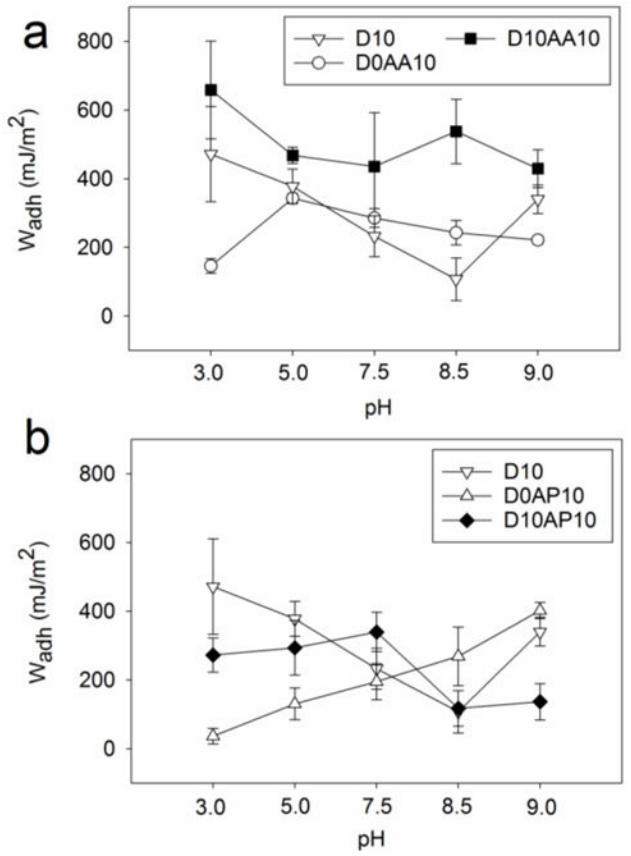

Figure 4.

Work of adhesion (W_{adh}) of adhesive hydrogels containing anionic AAc (a) and cationic APMH (b) tested against a wetted APTS-functionalized glass substrate at pH 3.0-9.0 (n = 3). Refer to Tables S6-S8 for results of statistical analysis.

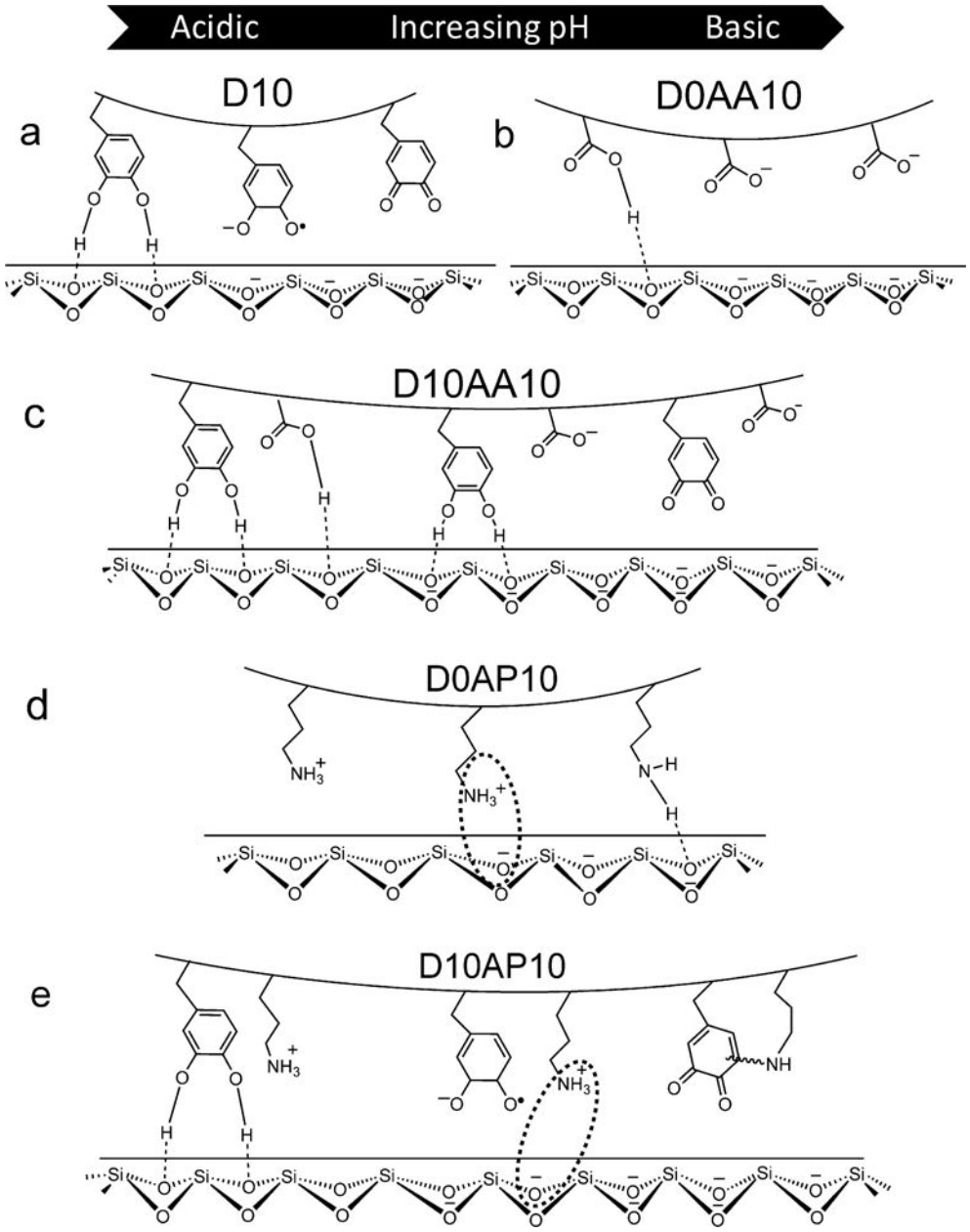

Scheme 1.

Schematic representation of adhesive hydrogels D10 (a), D10AA10 (b), D0AP10 (c) and D10AP10 (d) interacting with a wetted quartz substrate at pH ranging from 3.0 to 9.0 (from left to right).

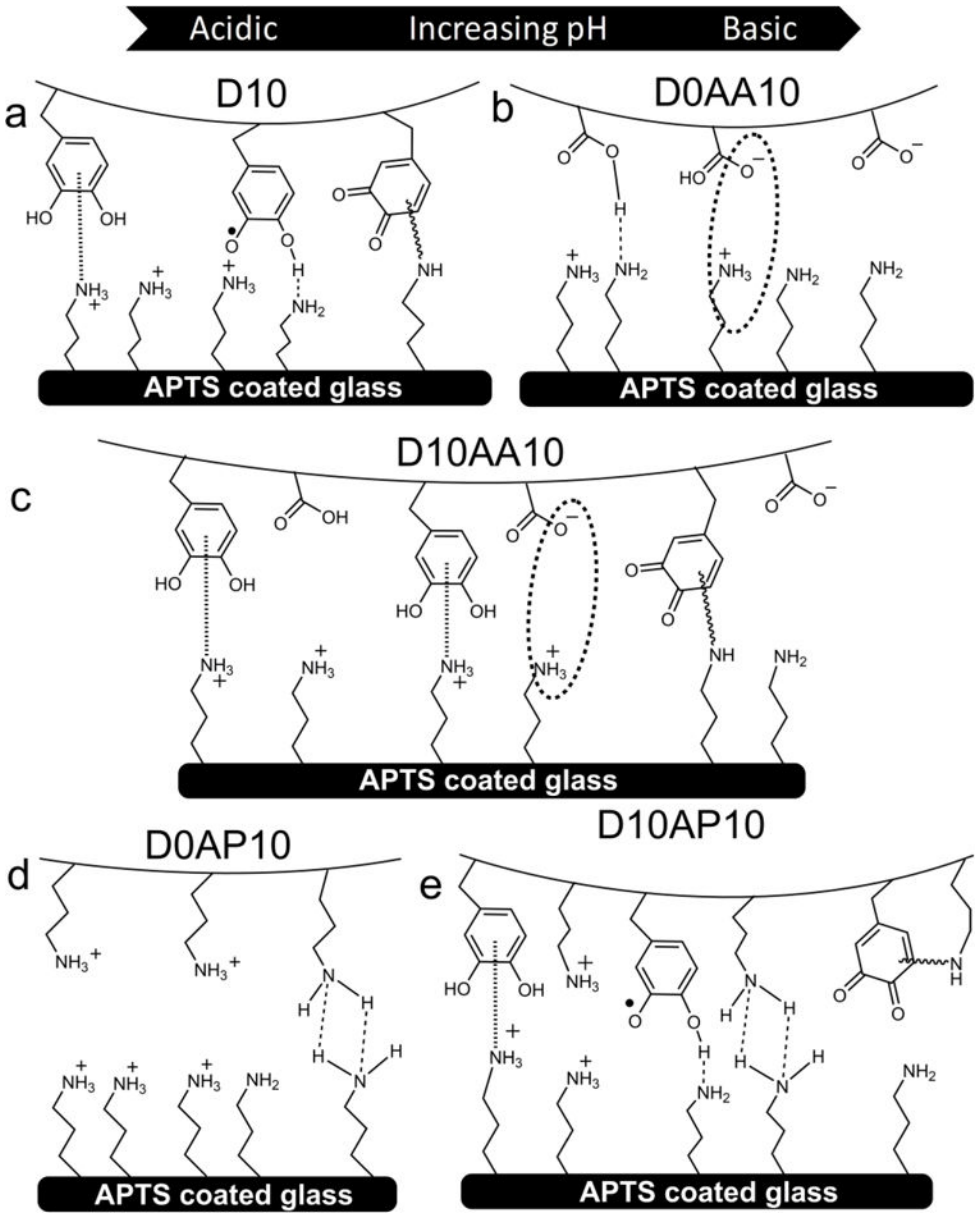

Scheme 2.

Schematic representation of adhesive hydrogels D10 (a), D0AA10 (b), D10AA10 (c), D0AP10 (d) and D10AP10 (e) interacting with a wetted amine-functionalized substrate (APTS-coated glass) at pH ranging from 3.0 to 9.0 (from left to right).